Koopman Operator Based Modeling and Control of Rigid Body Motion Represented by Dual Quaternions

Vrushabh Zinage Efstathios Bakolas

Abstract— **In this paper, we systematically derive a finite set of Koopman based observables to construct a lifted linear state space model that describes the rigid body dynamics based on the dual quaternion representation. Methods such as the Extended Dynamic Mode Decomposition (EDMD) can compute finite approximations of the Koopman operator for different classes of problems but in general, they cannot offer guarantees that the computed approximation of the nonlinear dynamics is sufficiently accurate unless an appropriate set of observables is available. State-of-the-art methods in the field compute approximations of the observables by using neural networks, standard radial basis functions (RBFs), polynomials or heuristic approximations of these functions. However, these observables might not yield a sufficiently accurate approximation of the dynamics. In contrast, we first show the pointwise convergence of the derived observable functions to zero. Next, we use the derived observables in EDMD to compute the lifted linear state and input matrices for the rigid body dynamics. Finally, we show that an LQR type (linear) controller, which is designed based on the truncated linear state space model, can steer the rigid body to a desired state while its performance is commensurate with that of a nonlinear controller. The efficacy of our approach is demonstrated through numerical simulations.**

I. Introduction

We consider the problem of modeling and control of the dual quaternion based representation of rigid body motion using the Koopman operator framework. In particular, we propose a systematic way to describe the rigid body dynamics in terms of a linear system which is defined over a *lifted* state space spanned by the so-called Koopman based observables. The main advantage of utilizing the Koopman operator is that it explicitly accounts for nonlinearities in the dynamics unlike methods which rely on (local) linearization of the (nonlinear) dynamics about a point. However the lifted state space is in general infinite-dimensional and thus any meaningful finite-dimensional approximation (truncation) of the lifted state space will have higher dimension than the original nonlinear system model. The states of the lifted (linear) model are (nonlinear) functions of the states of the original (nonlinear) system which are known as observables. Unfortunately, there are systematic methods for the characterization of observables for general nonlinear systems. In this paper, we derive in a systematic way a set of observables for the rigid body motion described in terms of dual quaternions and we subsequently propose simple linear control design techniques based on the lifted linear system associated with the latter observable. It turns out that these linear controllers perform similarly with a benchmark nonlinear controller for this particular system.

This research has been supported in part by NSF award CMMI-1937957.
Vrushabh Zinage (graduate student) and Efstathios Bakolas (Associate Professor) are with the Department of Aerospace Engineering and Engineering Mechanics, The University of Texas at Austin, Austin, Texas 78712-1221, USA, Emails:vrushabh.zinage@utexas.edu; bakolas@austin.utexas.edu

Literature review: The motion of a rigid body (position and attitude) can be represented in a compact manner through dual quaternions. This representation, takes automatically into account the natural coupling between the rotation and translation of a rigid body which thereby allows us to design a single controller which can control both the attitude and position of the rigid body simultaneously. Dual quaternions have been successfully applied to rigid body control [1]–[6], manipulator robots [7], inverse kinematic analysis, spacecraft formation flying [8], [9], and computer vision.

In recent years, Koopman operator has drawn attention among the controls and robotics community [10]–[12]. Identification of Koopman-invariant subspaces using neural networks has been explored in [13]–[15] and using data-driven approaches in [16]–[18]. Extensions of these results / methods for robotic applications can be found in [19]–[22], control synthesis [23]–[25], aerospace applications [26], [27], power systems [28], [29], control of PDEs [30] and climate research [31]. The major challenge in using Koopman operator methods is the characterization of the observable functions. State-of-the-art methods in the field, rely on heuristics or they try to learn these functions by using machine learning tools [19], [32]. The main advantage of using Koopman operator based techniques for modeling and control of dual quaternion based rigid body motion is two-fold. First, unlike linear models obtained through linearization about a fixed point whose accuracy is restricted in the vicinity of the latter point, the lifted linear model obtained by applying Koopman operator techniques provides an accurate description of the dynamics of the original system throughout a large subset of (if not the whole) the state space of the original system. Second, the availability of versatile and robust tools for analysis and control of linear systems make the analysis and control of the rigid body motion much easier.

Main contributions: In this paper, we provide a systematic method to derive and construct the observable functions for the rigid body dynamics based on the dual quaternion representation. We show that these observables are functions of the dual quaternions which can form a sequence of functions. We prove that the latter sequence converges pointwise to the zero function. This result essentially allow us to truncate the proposed sequence of observables and obtain a finite-dimensional linear approximation of the rigid body dynamics which is sufficiently accurate for modeling and control design purposes. Further, we use these observables to design a data-driven Koopman based LQR controller for setpoint tracking. Through numerical simulations, we compare the efficacy of the proposed linear controller with a nonlinear controller [33] and show that our controller shows equivalent performance and is able to steer the rigid body to the desired state.

Structure of the paper: In Section II, we introduce the quaternion and dual quaternion algebra followed by the nonlinear rigid body dynamics. Subsequently, we provide an overview of the Koopman operator. In Section III, we provide the derivation of the set of observables that will induce the lifted linear state space model by using EDMD. In Section V, we design a data-driven Koopman based LQR controller. Numerical simulations are presented in Section VI, and finally Section VII presents concluding remarks.

II. Preliminaries

A. Quaternion Algebra

A quaternion q can be represented by a pair $(\bar{q}, q_4)$ where $\bar{q} \in \mathbb{R}^3$ is known as its vector part and $q_4 \in \mathbb{R}$ as its scalar part. The set of quaternions is denoted by $\mathbb{Q}$. Some of the basic operations on quaternions are given below [33], [34]:
Addition: $a + b = (\bar{a} + \bar{b}, a_4 + b_4)$,
Multiplication by a scalar: $\lambda a = (\lambda \bar{a}, \lambda a_4)$,
Multiplication: $ab = (a_4 \bar{b} + b_4 \bar{a} + \bar{a} \times \bar{b}, a_4 b_4 - \bar{a} \cdot \bar{b})$
Conjugation: $a^\star = (-\bar{a}, a_4)$,
Dot product: $a \cdot b = \frac{1}{2}(a^\star b + b^\star a) = \frac{1}{2}(ab^\star + ba^\star) = (\bar{0}, a_4 b_4 + \bar{a} \cdot \bar{b})$,
Cross product: $a \times b = \frac{1}{2}(ab - b^\star a^\star) = (b_4 \bar{a} + a_4 \bar{b} + \bar{a} \times \bar{b}, 0)$,
Norm: $\|a\|^2 = aa^\star = a^\star a = a \cdot a = (\bar{0}, a_4^2 + \bar{a} \cdot \bar{a})$,
where $a, b \in \mathbb{Q}$.

B. Dual Quaternion Algebra

A dual quaternion $\widehat{q}$ can be represented by a pair (q_r, q_d) where $q_r, q_d \in \mathbb{Q}$ and q_r and q_d are the real and dual parts of $\widehat{q}$, respectively. Let the set of dual quaternions be denoted by $\mathbb{D}$. The dual quaternion $\widehat{q}$ can also be represented as $\widehat{q} = q_r + \epsilon q_d$ where $\epsilon^2 = 0$ and $\epsilon \neq 0$. A list of some basic operations on dual quaternions are given below [33], [34]:
Addition: $\widehat{a} + \widehat{b} = (a_r + b_r) + \epsilon (a_d + b_d)$,
Multiplication by a scalar: $\lambda \widehat{a} = (\lambda a_r) + \epsilon (\lambda a_d)$,
Multiplication: $\widehat{a}\widehat{b} = (a_r b_r) + \epsilon (a_r b_d + a_d b_r)$,
Conjugation: $\widehat{a}^\star = a_r^\star + \epsilon a_d^\star$,
Swap: $\widehat{a}^{\rm s} = a_d + \epsilon a_r$,
Dot product: $\widehat{a} \cdot \widehat{b} = \frac{1}{2}\left(\widehat{a}^\star \widehat{b} + \widehat{b}^\star \widehat{a}\right) = \frac{1}{2}\left(\widehat{a}\widehat{b}^\star + \widehat{b}\widehat{a}^\star\right)$
$= a_r \cdot b_r + \epsilon (a_d \cdot b_r + a_r \cdot b_d)$,
Cross product: $\widehat{a} \times \widehat{b} = \frac{1}{2}\left(\widehat{a}\widehat{b} - \widehat{b}^\star \widehat{a}^\star\right)$
$= a_r \times b_r + \epsilon (a_d \times b_r + a_r \times b_d)$,
Circle product: $\widehat{a} \circ \widehat{b} = a_r \cdot b_r + a_d \cdot b_d$,
Norm: $\|\widehat{a}\|^2 = a_r \cdot a_r + a_d \cdot a_d$,
Dual norm: $\|\widehat{a}\|_d^2 = \widehat{a}\widehat{a}^\star = \widehat{a}^\star \widehat{a} = \widehat{a} \cdot \widehat{a}$
$= (a_r \cdot a_r) + \epsilon (2 a_r \cdot a_d)$,
Multiplication by matrix : $M \star \widehat{q} = (M_{11} \star q_r + M_{12} \star q_d) + \epsilon (M_{21} \star q_r + M_{22} \star q_d)$ with $\widehat{a}, \widehat{b} \in \mathbb{D}$ and $M = \begin{bmatrix} M_{11} & M_{12} \\ M_{21} & M_{22} \end{bmatrix} \in \mathbb{R}^{8 \times 8}$, where $M_{11}, M_{12}, M_{21}, M_{22} \in \mathbb{R}^{4 \times 4}$.

C. Kinematics of rigid body in terms of dual quaternions

The kinematics of the rigid body in terms of the dual quaternions can be written as follows:

$$\dot{\widehat{q}} = \frac{1}{2}\widehat{q}\widehat{\omega}^B = \frac{1}{2}\widehat{\omega}^E \widehat{q}, \tag{1}$$

where $\widehat{\omega}^B = \omega^B + \epsilon v^B$, $\widehat{\omega}^E = \omega^E + \epsilon v^E$, $\widehat{q} = q_r + \epsilon q_d = q + \epsilon \frac{1}{2} q t^B$, q is the rotation quaternion, $t^B = (\bar{t}^B, 0)$, $\bar{t}^B$ is the translation vector in the body frame and superscript B and E denotes the body and inertial frame respectively. Further, $\omega^B = (\bar{\boldsymbol{\omega}}, 0) \in \mathbb{Q}$ and $v^B = (\bar{\boldsymbol{v}}, 0) \in \mathbb{Q}$ where $\bar{\boldsymbol{\omega}} \in \mathbb{R}^3$ and $\bar{\boldsymbol{v}} \in \mathbb{R}^3$ are the angular and linear velocities of the rigid body in the body frame respectively.

D. Dynamics of rigid body in terms of dual quaternions

The rigid body dynamics in terms of dual quaternions can be written as follows [34]:

$$M^B \star (\dot{\widehat{\omega}}^B)^s = \widehat{F}^B - \widehat{\omega}^B \times (M^B \star ((\widehat{\omega}^B)^s)) \tag{2}$$

where $(\cdot)^s$ denotes the swap operation performed on $(\cdot)$, M^B is the dual inertia matrix, $\widehat{F}^B = F^B + \epsilon \tau^B$ is the dual force applied to the center of mass of the body, $F^B = (\bar{F}^B, 0)$ and $\tau = (\bar{\tau}, 0)$. Consider a modified control input $\widehat{u} = \widehat{F}^B - \widehat{\omega}^B \times (M^B \star ((\widehat{\omega}^B)^s))$. Then (2) becomes

$$\dot{\widehat{\omega}}^B = (M^{B(-1)} \star \widehat{u})^s, \tag{3}$$

where $M^B \in \mathbb{R}^{8 \times 8}$ is a block matrix

$$M^B = \begin{bmatrix} mI_3 & 0_{3\times1} & 0_{3\times3} & 0_{3\times1} \\ 0_{1\times3} & 1 & 0_{1\times3} & 0 \\ 0_{3\times3} & 0_{3\times1} & \bar{I}^B & 0_{3\times1} \\ 0_{1\times3} & 0 & 0_{1\times3} & 1 \end{bmatrix},$$

where $\bar{I}^B \in \mathbb{R}^{3\times3}$ is the mass moment of inertia (positive definite matrix) and m is the mass of the body.

Remark 1. A dual quaternion $\widehat{q}$ can also be represented in a vector form as $\widehat{q} = [\bar{q}_r \;\; q_{r4} \;\; \bar{q}_d \;\; q_{d4}]^{\rm T}$.

To keep the notation simple, the superscript B for body frame will be dropped.

E. Koopman Operator

In this section, we briefly review the key concepts from the Koopman operator theory. To this end, consider a continuous-time nonlinear dynamical system $\dot{\boldsymbol{x}} = f(\boldsymbol{x})$. where $\boldsymbol{x} \in \mathbb{R}^n$ and the vector field f is assumed to satisfy regularity assumptions that ensure existence and uniqueness of solutions. Let $\mathcal{O}$ be the set of observables (functions of the system's state) $\psi : \mathbb{R}^n \to \mathbb{C}$ where $\mathbb{C}$ belongs to the set of complex numbers. The Koopman operator $\mathcal{K}_t : \mathcal{O} \to \mathcal{O}$ associated with system $\dot{\boldsymbol{x}} = f(\boldsymbol{x})$ is defined as $[\mathcal{K}_t \psi(\boldsymbol{x})] = \mathcal{K}_t(\psi(\boldsymbol{x}))$. Although the underlying dynamics is, in general, nonlinear, the Koopman operator is a linear infinite dimensional operator which acts on the space of observables. In particular, it holds that

$$[\mathcal{K}_t(\alpha\psi_1(\boldsymbol{x}) + \beta\psi_2(\boldsymbol{x}))] = \alpha[\mathcal{K}_t\psi_1](\boldsymbol{x}) + \beta[\mathcal{K}_t\psi_2](\boldsymbol{x}),$$

where ψ_1, $\psi_2 \in \mathcal{O}$ and α, $\beta \in \mathbb{C}$. A Koopman eigenfunction $\psi_\lambda(\boldsymbol{x}) \in \mathcal{O}$ corresponding to an eigenvalue $\lambda \in \mathbb{C}$ is defined as $[\mathcal{K}_t \psi_\lambda(\boldsymbol{x})] = \lambda \psi_\lambda(\boldsymbol{x})$, which implies that $\psi_\lambda(\boldsymbol{x})$ satisfies the differential equation $\dot{\psi}_\lambda(\boldsymbol{x}) = \lambda \psi_\lambda(\boldsymbol{x})$. For a controlled system of the form $\dot{\boldsymbol{x}} = f(\boldsymbol{x}) + B\boldsymbol{u}$ with input matrix $B \in \mathbb{R}^{n\times m}$ and control input $\boldsymbol{u} \in \mathbb{R}^m$, the dynamics of the Koopman eigenfunctions become

$$\dot{\psi}_\lambda(\boldsymbol{x}) = \lambda\psi_\lambda(\boldsymbol{x}) + \nabla\psi_\lambda(\boldsymbol{x}) B\boldsymbol{u} \tag{4}$$

The Koopman operator $\mathcal{K}_d$ for discrete nonlinear system $\boldsymbol{x}_{k+1} = h(\boldsymbol{x}_k)$ can be written in terms of $\mathcal{K}$ and the sampling time T as $\mathcal{K} = \log(\mathcal{K}_d)/T$. Consequently, $\psi(\boldsymbol{x}_{k+1}) = \mathcal{K}_d \psi(\boldsymbol{x}_k)$. In general it is not possible to find the set of finite Koopman eigenfunctions for any nonlinear dynamics. In practice, one has to use a finite subspace approximation of the Koopman operator $\bar{\mathcal{K}}_d \in \mathbb{R}^N \times \mathbb{R}^N$ which acts on a subspace $\mathcal{S} \subset \mathcal{O}$. If the finite set of observables are given by $\boldsymbol{z}(\boldsymbol{x}) = [\psi_1(\boldsymbol{x}) \;\; \psi_2(\boldsymbol{x}) \ldots \psi_N(\boldsymbol{x})]^{\rm T} \in \mathbb{R}^N$, then

$\boldsymbol{z}(\boldsymbol{x}_{k+1}) \approx \bar{\mathcal{K}}_d \boldsymbol{z}(\boldsymbol{x}_k)$ approximation holds true. Given the data $\mathcal{D} = \{\boldsymbol{x}_k\}_{k=0}^{d}$, $\bar{\mathcal{K}}_d$ can be computed by solving the following least squares minimization problem:

$$\min_{\bar{\mathcal{K}}_d} \|\boldsymbol{z}(\boldsymbol{x}_{k+1}) - \bar{\mathcal{K}}_d \boldsymbol{z}(\boldsymbol{x}_k)\|_2^2. \tag{5}$$

Consider the discrete-time controlled system $\boldsymbol{x}_{k+1} = h(\boldsymbol{x}_k, \boldsymbol{u}_k)$. Then, the Koopman operator $\mathcal{K}_d$ over the extended state space $\mathbb{G} : \mathcal{X} \times \mathcal{U}$ and observable $g(\boldsymbol{x}_k, \boldsymbol{u}_k) = [\boldsymbol{z} \quad v(\boldsymbol{x}_k, \boldsymbol{u}_k)]^{\mathrm{T}}$ can be defined as $g(\boldsymbol{x}_{k+1}, \boldsymbol{u}_{k+1}) = \mathcal{K}_d g(\boldsymbol{x}_k, \boldsymbol{u}_k)$ [19].

III. Derivation of Koopman based observables

In this section, we provide a systematic way to derive the observable functions for the continuous-time rigid body motion based on the dual quaternion representation.

Theorem 1. For the nonlinear system governed by (1) and (2), the lifted state space $\boldsymbol{z}$ is spanned by the following set of observable functions

$$\boldsymbol{z} = (\widehat{q},\ \widehat{\omega},\ \{\widehat{f}_k\}_0^{\infty}), \tag{6}$$

where $\widehat{f}_k = \widehat{q}\widehat{\omega}^k$.

Proof. Let $\widehat{\omega}^{B(k)}$ be defined as $\widehat{\omega}^{B(k)} = \underbrace{(\widehat{\omega}^B(\widehat{\omega}^B(\ldots(\widehat{\omega}^B\widehat{\omega}^B)}_{k \text{ times}}\ldots)))$. Let $f_1 = \widehat{q}\widehat{\omega}^B$. Then,

$$\begin{aligned}\dot{f}_1 &= \dot{\widehat{q}}\widehat{\omega}^B + \widehat{q}\dot{\widehat{\omega}}^B = \frac{1}{2}(\widehat{q}\widehat{\omega}^B)\widehat{\omega}^B + \widehat{q}\dot{\widehat{\omega}}^B \\ &= \frac{1}{2}\widehat{q}(\widehat{\omega}^B\widehat{\omega}^B) + \widehat{q}\dot{\widehat{\omega}}^B = \frac{1}{2}\widehat{q}\widehat{\omega}^{B(2)} + \widehat{q}\dot{\widehat{\omega}}^B,\end{aligned}$$

where $\widehat{\omega}^{B(2)} = \widehat{\omega}^B\widehat{\omega}^B$. Now let $f_2 = \widehat{q}\widehat{\omega}^{B(2)}$. Then,

$$\begin{aligned}\dot{f}_2 &= \dot{\widehat{q}}\widehat{\omega}^{B(2)} + \widehat{q}\dot{\widehat{\omega}}^{B(2)} = \frac{1}{2}(\widehat{q}\widehat{\omega}^B)\widehat{\omega}^{B(2)} + \widehat{q}\dot{\widehat{\omega}}^B \\ &= \frac{1}{2}\widehat{q}(\widehat{\omega}^B\widehat{\omega}^{B(2)}) + \widehat{q}\dot{\widehat{\omega}}^B = \frac{1}{2}\widehat{q}\widehat{\omega}^{B(3)} + \widehat{q}\dot{\widehat{\omega}}^B,\end{aligned} \tag{7}$$

where $\widehat{\omega}^{B(3)} = \widehat{\omega}^B(\widehat{\omega}^B\widehat{\omega}^B)$. Therefore, in general

$$\dot{f}_k = \frac{1}{2}f_{k+1} + \sum_{i=1}^{k} \widehat{\omega}^{B(i-1)}(M^{-1} \star \tilde{\boldsymbol{u}})\widehat{\omega}^{B(k-i)}. \tag{8}$$

As $N \to \infty$, we obtain countably infinite collection of observables given by (6). □

In the following we derive the general expression for $\widehat{\omega}^{B(k)}$ which will be used in subsequent analysis.

A. General expression for $\widehat{\omega}^{B(k)}$

Consider the expression for $\widehat{\omega}_1^B := \widehat{\omega}^B\widehat{\omega}^B$,

$$\widehat{\omega}^B\widehat{\omega}^B = (\omega^B\omega^B) + \epsilon(\omega^B v^B + v^B\omega^B). \tag{9}$$

Now, $(\omega^B\omega^B), \omega^B v^B$ and $v^B\omega^B$ can be written as

$$\begin{aligned}\omega^B\omega^B &= (\bar{\boldsymbol{\omega}}^B \times \bar{\boldsymbol{\omega}}^B, -\bar{\boldsymbol{\omega}}^B.\bar{\boldsymbol{\omega}}^B) = (0, -|\bar{\boldsymbol{\omega}}^B|^2) \\ \omega^B v^B &= (\bar{\boldsymbol{\omega}}^B \times \bar{\boldsymbol{v}}^B, -\bar{\boldsymbol{\omega}}^B.\bar{\boldsymbol{v}}^B), \\ v^B\omega^B &= (\bar{\boldsymbol{v}}^B \times \bar{\boldsymbol{\omega}}^B, -\bar{\boldsymbol{\omega}}^B.\bar{\boldsymbol{v}}^B).\end{aligned}$$

Therefore, $\widehat{\omega}^B\widehat{\omega}^B = (0, -|\bar{\boldsymbol{\omega}}^B|^2) + \epsilon(\bar{0}, -2\bar{\boldsymbol{\omega}}^B.\bar{\boldsymbol{v}}^B)$. Now, the expression of $\widehat{\omega}^B\widehat{\omega}_1^B = \widehat{\omega}^B\widehat{\omega}^B\widehat{\omega}^B$ can be written as

$$\widehat{\omega}^B\widehat{\omega}_1^B = \omega^B\omega_1^B + \epsilon(\omega_1^B v^B + v_1^B\omega^B). \tag{10}$$

Now, $\omega^B\omega_1^B, \omega_1^B v^B$ and $v_1^B\omega^B$ in (10) are given as

$$\begin{aligned}&\omega^B\omega_1^B = (-|\bar{\boldsymbol{\omega}}^{B(2)}|\bar{\boldsymbol{\omega}}^B, 0), \quad \omega_1^B v^B = (-|\bar{\boldsymbol{\omega}}^{B(2)}|\bar{\boldsymbol{v}}^B, 0), \\ &v_1^B\omega^B = (-2(\bar{\boldsymbol{\omega}}^B.\bar{\boldsymbol{v}}^B)\bar{\boldsymbol{\omega}}^B, 0),\end{aligned}$$

Therefore

$$\begin{aligned}\widehat{\omega}_2^B := \widehat{\omega}^B\widehat{\omega}_1^B =& (-|\bar{\boldsymbol{\omega}}^{B(2)}|\bar{\boldsymbol{\omega}}^B, 0) + \epsilon(-|\bar{\boldsymbol{\omega}}^{B(2)}|\bar{\boldsymbol{v}}^B - \\ & 2(\bar{\boldsymbol{\omega}}^B.\bar{\boldsymbol{v}}^B)\bar{\boldsymbol{\omega}}^B, 0)\end{aligned}$$

Now, the expression of $\widehat{\omega}_3^B := \widehat{\omega}^B\widehat{\omega}_2^B$ is given by

$$\widehat{\omega}^B\widehat{\omega}_2^B = (\omega^B\omega_2^B) + \epsilon(\omega_2^B v^B + v_2^B\omega^B) \tag{11a}$$

$$\omega^B\omega_2^B = (0, -|\bar{\boldsymbol{\omega}}^B|^4) \tag{11b}$$

$$\omega_2^B v^B = (|\bar{\boldsymbol{\omega}}^B|^2(\bar{\boldsymbol{\omega}}^B \times \bar{\boldsymbol{v}}^B), -|\bar{\boldsymbol{\omega}}^B|^2((\bar{\boldsymbol{\omega}}^B.\bar{\boldsymbol{v}}^B))) \tag{11c}$$

$$v_2^B\omega^B = (-|\bar{\boldsymbol{\omega}}^B|^2(\bar{\boldsymbol{\omega}}^B \times \bar{\boldsymbol{v}}^B), -|\bar{\boldsymbol{\omega}}^B|^2\bar{\boldsymbol{\omega}}^B.\bar{\boldsymbol{v}}^B - 2(\bar{\boldsymbol{\omega}}^B.\bar{\boldsymbol{v}}^B)^2) \tag{11d}$$

Therefore, from (11)

$$\widehat{\omega}_3^B = (0, -|\bar{\boldsymbol{\omega}}^B|^4) + \epsilon(0, -2|\bar{\boldsymbol{\omega}}^B|^2\bar{\boldsymbol{\omega}}^B.\bar{\boldsymbol{v}}^B - 2(\bar{\boldsymbol{\omega}}^B.\bar{\boldsymbol{v}}^B)^2)$$

Again, let $\widehat{\omega}_4^B := \widehat{\omega}^B\widehat{\omega}_3^B$. Then,

$$\widehat{\omega}^B\widehat{\omega}_3^B = (\omega^B\omega_3^B) + \epsilon(\omega_3^B v^B + v_3^B\omega^B), \tag{12a}$$

$$\omega_3^B\omega^B = (-|\bar{\boldsymbol{\omega}}^B|^4\bar{\boldsymbol{\omega}}^B, 0),\ \omega_3^B v^B = (-|\bar{\boldsymbol{\omega}}^B|^4\bar{\boldsymbol{v}}^B, 0) \tag{12b}$$

$$v_3^B\omega^B = (-2|\bar{\boldsymbol{\omega}}^B|^2(\bar{\boldsymbol{\omega}}^B.\bar{\boldsymbol{v}}^B)\bar{\boldsymbol{\omega}}^B - 2(\bar{\boldsymbol{\omega}}^B.\bar{\boldsymbol{v}}^B)^2\bar{\boldsymbol{\omega}}^B, 0). \tag{12c}$$

Therefore, from (12)

$$\begin{aligned}\widehat{\omega}_4^B := \widehat{\omega}^B\widehat{\omega}_3^B =& (-|\bar{\boldsymbol{\omega}}^B|^4\bar{\boldsymbol{\omega}}^B, 0) + \epsilon(-|\bar{\boldsymbol{\omega}}^B|^4\bar{\boldsymbol{v}}^B - \\ & 2|\bar{\boldsymbol{\omega}}^B|^2(\bar{\boldsymbol{\omega}}^B.\bar{\boldsymbol{v}}^B)\bar{\boldsymbol{\omega}}^B - 2(\bar{\boldsymbol{\omega}}^B.\bar{\boldsymbol{v}}^B)^2\bar{\boldsymbol{\omega}}^B, 0).\end{aligned}$$

Hence, the value of $\widehat{\omega}^{B(k)}$ can be written as follows:

- Case 1: k is odd

$$\begin{aligned}\widehat{\omega}^{B(k)} =& (|\bar{\boldsymbol{\omega}}^B|^{k-1}\bar{\boldsymbol{\omega}}^B, 0) + \epsilon(-|\bar{\boldsymbol{\omega}}^B|^{(k-1)}\bar{\boldsymbol{v}}^B - \\ & 2\sum_{i=1}^{\frac{k-1}{2}} |\bar{\boldsymbol{\omega}}^B|^{(k-1-2i)}(\bar{\boldsymbol{\omega}}^B.\bar{\boldsymbol{v}}^B)^i\bar{\boldsymbol{\omega}}^B, 0)\end{aligned}$$

- Case 2: k is even

$$\widehat{\omega}^{B(k)} = (\bar{0}, -|\bar{\boldsymbol{\omega}}^B|^k) + \epsilon(\bar{0}, -2\sum_{i=1}^{k/2} |\bar{\boldsymbol{\omega}}^B|^{(k-2i)}(\bar{\boldsymbol{\omega}}^B.\bar{\boldsymbol{v}}^B)^i)$$

The following lemma will be used to prove the pointwise convergence of the observables to zero.

Lemma 1. For any $\widehat{a}, \widehat{b} \in \mathbb{D}$, we have

$$\|\widehat{a}\widehat{b}\| \leq \sqrt{3/2}\|\widehat{a}\|\|\widehat{b}\|. \tag{13}$$

Proof. Refer to the proof of Lemma 1 from [34]. □

Assumption 1. We assume that the maximum angular and linear velocities of the rigid body are constrained and are known a-priori. In other words, there exists some $\bar{\boldsymbol{\omega}}_0$ and $\bar{\boldsymbol{v}}_0$ such that $\omega_0 > \max_{\bar{\boldsymbol{\omega}}}(|\bar{\boldsymbol{\omega}}|)$ and $v_0 > \max_{\bar{\boldsymbol{v}}}(|\bar{\boldsymbol{v}}|)$.

Now, let us consider the normalized angular and linear velocities which are defined as follows:

$$\|\tilde{\bar{\boldsymbol{\omega}}}\| = \frac{\|\bar{\boldsymbol{\omega}}\|}{\mathtt{max}(\{\omega_0, v_0\})} < 1, \quad \|\tilde{\bar{\boldsymbol{v}}}\| = \frac{\|\bar{\boldsymbol{v}}\|}{\mathtt{max}(\{\omega_0, v_0\})} < 1$$

Next, we define the modified observable function $\widehat{f}_k$ as $\widehat{f}_k = \widehat{q}\tilde{\widehat{\omega}}^k$ where $\tilde{\widehat{\omega}} = (\tilde{\bar{\boldsymbol{\omega}}}, 0) + \epsilon(\tilde{\bar{\boldsymbol{v}}}, 0)$. The expression of $\widehat{f}_k$ can be written in terms of f_k as $\widehat{f}_k = (\widehat{\omega}_0)^k f_k$ where $\widehat{\omega}_0 = (0, \mathtt{max}(\{\omega_0, v_0\})) + \epsilon(\bar{0}, 0)$. The linear dynamics in the lifted space can then be written as follows:

$$\dot{\widehat{f}}_k = \widehat{\omega}_0 \widehat{f}_{k+1} + \widehat{q} \sum_{i=1}^{k} \tilde{\widehat{\omega}}^{B(i-1)} (M^{-1} \star \tilde{\boldsymbol{u}})^s \tilde{\widehat{\omega}}^{B(k-i)} \tag{14}$$

In addition, let

$$B_k := \sum_{i=1}^{k} \tilde{\widehat{\omega}}^{B(i-1)} (M^{-1} \star \tilde{\boldsymbol{u}})^s \tilde{\widehat{\omega}}^{B(k-i)} \tag{15}$$

Next we consider the sets $\mathcal{D}_{\widehat{\omega}}$ and $\mathcal{D}_{\widehat{v}}$ where

$$\mathcal{D}_{\widehat{\omega}} := \{\tilde{\widehat{\omega}} : \|\tilde{\bar{\boldsymbol{\omega}}}\| < 1\}, \quad \mathcal{D}_{\widehat{v}} := \{\tilde{\widehat{v}} : \|\tilde{\bar{\boldsymbol{v}}}\| < 1\}$$

Lemma 2. For $k \in [2, N]_d$, the following holds true:

$$\lim_{\mathtt{max}(\{\omega_0, v_0\}) \to \infty} B_k = \widehat{0}, \quad \lim_{k \to \infty} B_k = \widehat{0} \tag{16}$$

Proof. Since $\tilde{\widehat{\omega}} = [(\bar{\boldsymbol{\omega}}, 0) + \epsilon(\bar{\boldsymbol{v}}, 0)]/\mathtt{max}(\{\omega_0, v_0\})$. Therefore $\lim_{\mathtt{max}(\{\omega_0, v_0\}) \to \infty} \tilde{\widehat{\omega}} = (\bar{\mathbf{0}}, 0) + \epsilon(\bar{\mathbf{0}}, 0)$. Subsequently from (15), $\lim_{\omega_0 \to \infty} B_k = (\bar{0}, 0) + \epsilon(\bar{0}, 0)$ Further using Lemma 1,

$$\|B_k\| \leq \frac{3}{2} k \|\tilde{\widehat{\omega}}^{B(k-i)}\| \|(M^{-1} \star \tilde{\boldsymbol{u}})^s\| \tag{17}$$

Since $\lim_{k \to \infty} k x^k = 0$ for $x < 1$, taking limit on both sides of (17), we get $\lim_{k \to \infty} \|B_k\| = 0$. Consequently, $\lim_{k \to \infty} B_k = \widehat{0}$. This completes the proof. □

Remark 2. For higher value of ω_0, B_k (for all $k \in [2, N]_d$) can be approximated to be the zero dual number i.e. $B_k \approx (\bar{\mathbf{0}}, 0) + \epsilon(\bar{\mathbf{0}}, 0)$. In other words, as k and ω_0 increases, the dependence of the states on B_k decreases. Thereafter, the lifted space linear dynamics can be approximated as follows:

$$\dot{\widehat{f}}_1 = \widehat{\omega}_0 \widehat{f}_2 + \widehat{q}(M^{-1} \star \tilde{\boldsymbol{u}})^s / \omega_0, \tag{18a}$$

$$\dot{\widehat{f}}_k = \widehat{\omega}_0 \widehat{f}_{k+1} + \widehat{q} B_k, \qquad k \in [2, N]_d \tag{18b}$$

Theorem 2. For any $\boldsymbol{\omega} \in \mathcal{D}_{\widehat{\omega}}$ and $\boldsymbol{v} \in \mathcal{D}_{\widehat{v}}$, the sequences of functions $\widehat{f}_k$ and $\dot{\widehat{f}}_k$ converge pointwise to $\widehat{0}$, i.e.,

$$\lim_{k \to \infty} \widehat{f}_k = \widehat{0}, \quad \lim_{k \to \infty} \dot{\widehat{f}}_k = \widehat{0} \quad \forall\, \boldsymbol{\omega} \in \mathcal{D}_{\widehat{\omega}}, \ \ \boldsymbol{v} \in \mathcal{D}_{\widehat{v}}.$$

Proof. Since $\|\tilde{\bar{\boldsymbol{\omega}}}\| < 1$ and $\|\tilde{\bar{\tilde{\boldsymbol{v}}}}\| < 1$, we have

$$\lim_{k \to \infty} \|\tilde{\bar{\boldsymbol{\omega}}}^{B(k-1)}\| \tilde{\bar{\boldsymbol{\omega}}} = \mathbf{0}, \quad \lim_{k \to \infty} \|\tilde{\bar{\boldsymbol{\omega}}}^{B(k)}\| = 0. \tag{19}$$

In addition, we have

$$\sum_{i=1}^{k} \|\tilde{\bar{\boldsymbol{\omega}}}^B\|^{(k-2i)} (\tilde{\bar{\boldsymbol{\omega}}}^B . \tilde{\bar{\boldsymbol{v}}}^B)^i \leq \sum_{i=1}^{k} \|\tilde{\bar{\boldsymbol{\omega}}}^B\|^{(k-i)} \|\tilde{\bar{\boldsymbol{v}}}^B\|^{(i)} \tag{20}$$

Now, using the formula for the sum of geometric series, we have

$$\sum_{i=1}^{k} \|\tilde{\bar{\boldsymbol{\omega}}}^B\|^{(k-i)} \|\tilde{\bar{\boldsymbol{v}}}^B|^{(i)} = \frac{\|\tilde{\bar{\boldsymbol{\omega}}}^B|^{(k-1)} \|\tilde{\bar{\boldsymbol{v}}}^B\| (1 - (|\tilde{\bar{\boldsymbol{v}}}^B\| / \|\tilde{\bar{\boldsymbol{\omega}}}^B\|)^k)}{1 - \|\tilde{\bar{\boldsymbol{v}}}^B\| / \|\tilde{\bar{\boldsymbol{\omega}}}^B\|} \tag{21}$$

Taking limits on both sides of (21) gives

$$\lim_{k \to \infty} \sum_{i=1}^{k} \|\tilde{\bar{\boldsymbol{\omega}}}^B|^{(k-i)} \| \|\tilde{\bar{\boldsymbol{v}}}^B\|^{(i)} = 0. \tag{22}$$

Similarly, it can be shown that

$$\lim_{k \to \infty} \|\tilde{\bar{\boldsymbol{\omega}}}^B\|^{(k-1)} \tilde{\bar{\boldsymbol{v}}}^B + 2 \sum_{i=1}^{k} \|\tilde{\bar{\boldsymbol{\omega}}}^B\|^{(k-1-2i)} (\tilde{\bar{\boldsymbol{\omega}}}^B . \tilde{\bar{\boldsymbol{v}}}^B)^i \tilde{\bar{\boldsymbol{\omega}}}^B = \mathbf{0} \tag{23}$$

Using (19), (22) and (23), we conclude that $\lim_{k \to \infty} \tilde{\widehat{\omega}}^{B(k)} = (\bar{\mathbf{0}}, 0) + \epsilon(\bar{\mathbf{0}}, 0)$. Since $\widehat{f}_k = \widehat{q}\tilde{\widehat{\omega}}^{B(k)}$, using Lemma 2, we have

$$\|\widehat{q}\tilde{\widehat{\omega}}^{B(k)}\| \leq \sqrt{3/2} \|\widehat{q}\| \|\tilde{\widehat{\omega}}^{B(k)}\|. \tag{24}$$

Now, since $\lim_{k \to \infty} \|\tilde{\bar{\boldsymbol{\omega}}}^B\|^{(k)} = 0$, we have

$$\lim_{k \to \infty} \|\widehat{q}\tilde{\widehat{\omega}}^{B(k)}\| \leq 0 \implies \lim_{k \to \infty} \widehat{f}_k = \widehat{\mathbf{0}}.$$

Taking limits on both sides of (18b), we get $\lim_{k \to \infty} \dot{\widehat{f}}_k = \widehat{\mathbf{0}}$. Hence, the theorem is proved. □

Theorem 3. For any $\boldsymbol{\omega} \in \mathcal{D}_{\widehat{\omega}}$ and $\boldsymbol{v} \in \mathcal{D}_{\widehat{v}}$, it holds that

$$\|\widehat{f}_k\| > \|\widehat{f}_{k+1}\|, \quad k \in [2, N]_d \tag{25}$$

Proof. Since $\widehat{f}_k = \widehat{q}\tilde{\widehat{\omega}}^{B(k)}$, using Lemma 2, we have

$$\|\widehat{f}_{k+1}\|^2 \leq 3/2 \|\widehat{q}\tilde{\widehat{\omega}}^{B(k)}\|^2 \|\tilde{\widehat{\omega}}^B\|^2 = 3/2 \|\widehat{f}_k\|^2 \|\tilde{\widehat{\omega}}^B\|^2 \tag{26}$$

Therefore, $\|\tilde{\widehat{\omega}}^B\|^2 = (\bar{0}, |\tilde{\bar{\boldsymbol{\omega}}}|^2) + (\bar{0}, |\tilde{\bar{\boldsymbol{v}}}^2|) = (\bar{\mathbf{0}}, |\tilde{\bar{\boldsymbol{\omega}}}|^2 + |\tilde{\bar{\boldsymbol{v}}}^2|) < 2/3$. Hence, $\|\widehat{f}_{k+1}\|^2 \leq 3/2 \|\widehat{q}\tilde{\widehat{\omega}}^{B(k)}\|^2 \|\tilde{\widehat{\omega}}^B\|^2 < \|\widehat{f}_k\|^2$. Subsequently, $\|f_{k+1}\| < \|f_k\|$. Hence the theorem follows. □

IV. Lifted linear state space model

Based on the derived observables in Section III, the lifted state (from Theorem 1) is $\boldsymbol{z} = [\widehat{q}, \ \widehat{\omega}, \ \widehat{f}_1, \ldots \widehat{f}_N]^{\mathrm{T}}$. The lifted state space $\boldsymbol{z}$ is used to learn the lifted state and input matrices, A_{lift} and B_{lift} which is described as follows. First, from a random uniform distribution $[-1, 1]$,a set of random control inputs are chosen. These inputs are then applied sequentially to the discrete-time nonlinear system (**??**) with $\boldsymbol{x}_0$ as the initial state to get the subsequent states. Let the control input $\widehat{\boldsymbol{u}}_k$ be applied to take the rigid body from $\boldsymbol{x}_k$ to $\boldsymbol{x}_{k+1}$. Consequently, we construct the matrices $\boldsymbol{X} := [\boldsymbol{x}_0, \ldots, \boldsymbol{x}_{N_t-1}]$, $\boldsymbol{U} := [\widehat{\boldsymbol{u}}_0, \ldots, \widehat{\boldsymbol{u}}_{N_t-1}]$ and $\boldsymbol{Y} := [\boldsymbol{x}_1, \ldots, \boldsymbol{x}_{N_t}]$ where N_t+1 is the total number of data points collected. The matrix $\boldsymbol{Y}$ can be expressed as $\boldsymbol{Y} = \boldsymbol{h}(\boldsymbol{X}, \boldsymbol{U})$. Now given these matrices, A_{lift} and B_{lift}, can be computed via the solution to the following optimization problem

$$\min_{A_{\text{lift}}, B_{\text{lift}}} \quad \|\boldsymbol{Y}_{\text{lift}} - A_{\text{lift}} \boldsymbol{X}_{\text{lift}} - B_{\text{lift}} \boldsymbol{U}\|_F, \tag{27}$$

where $\boldsymbol{X}_{\text{lift}} = [\boldsymbol{z}(\boldsymbol{x}_0), \ldots, \boldsymbol{z}(\boldsymbol{x}_{N_t-1})]$ and $\boldsymbol{Y}_{\text{lift}} = [\boldsymbol{z}(\boldsymbol{x}_1), \ldots, \boldsymbol{z}(\boldsymbol{x}_{N_t})]$. The analytical solution to (27) is given

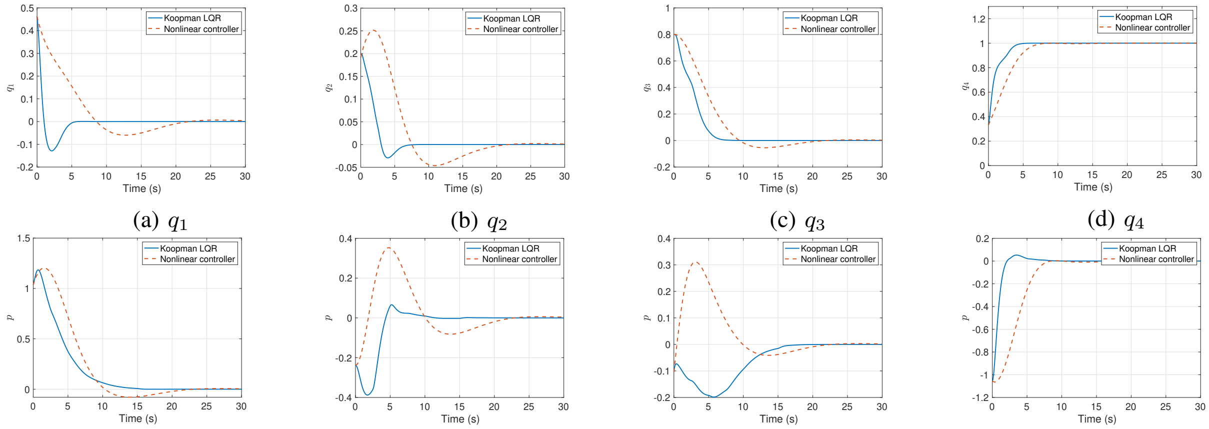

(a) q_1 (b) q_2 (c) q_3 (d) q_4

(e) q_5 (f) q_6 (g) q_7 (h) q_8

Fig. 1: Evolution of the dual quaternion $\widehat{q}$ with time

by $[A_{\text{lift}}, B_{\text{lift}}] = \boldsymbol{Y}_{\text{lift}}\ [\boldsymbol{X}_{\text{lift}}, \boldsymbol{U}]^{\dagger}$ where $(.)^{\dagger}$ denotes the Moore-Penrose pseudoinverse operator. Therefore, the lifted linear state space model is given by

$$\boldsymbol{z}_{k+1} = A_{\text{lift}}\boldsymbol{z}_k + B_{\text{lift}}\boldsymbol{u}_k. \tag{28}$$

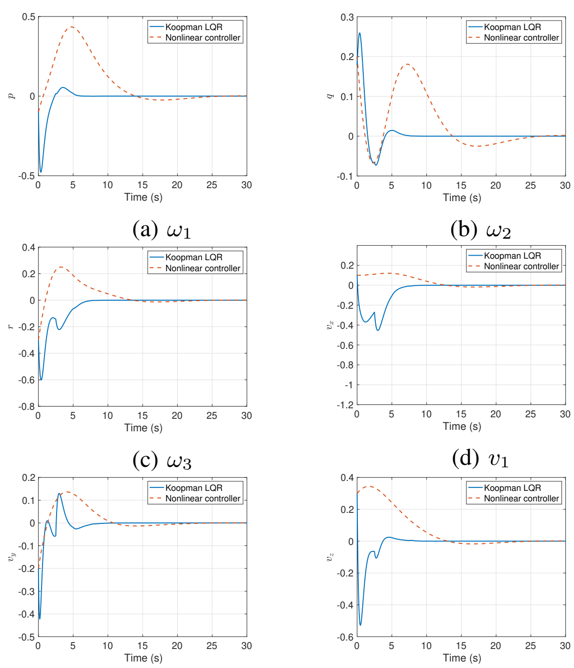

(a) ω_1 (b) ω_2

(c) ω_3 (d) v_1

(e) v_2 (f) v_3

Fig. 2: Angular and linear velocities v/s time

V. Linear Control Design using LQR

In this section, we design a LQR controller for the Koopman based on lifted state space model of the rigid body dynamics. Consider the lifted linear dynamics given by (28). The control design is based on the solution to the following infinite horizon LQR problem with performance index

$$J(\widehat{\boldsymbol{u}}_k) = \sum_{k=1}^{\infty} \boldsymbol{z}_k^{\mathrm{T}} Q_z \boldsymbol{z}_k + \widehat{\boldsymbol{u}}_k^{\mathrm{T}} R_z \widehat{\boldsymbol{u}}_k, \tag{29}$$

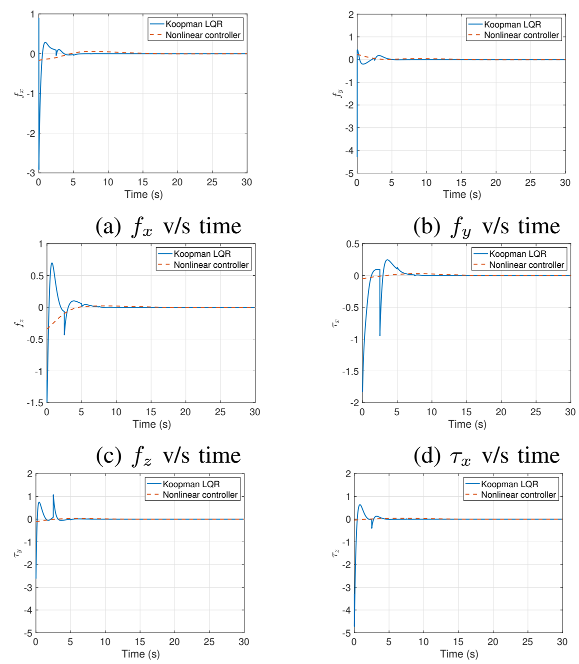

(a) f_x v/s time (b) f_y v/s time

(c) f_z v/s time (d) τ_x v/s time

(e) τ_y v/s time (f) τ_z v/s time

Fig. 3: Force $F^B = [f_x \quad f_y \quad f_z]^{\mathrm{T}}$ and torque $\tau^B = [\tau_x \quad \tau_y \quad \tau_z]^{\mathrm{T}}$ versus time t

where $Q_z = Q_z^{\mathrm{T}} \succcurlyeq 0$ and $R_z = R_z^{\mathrm{T}} \succ 0$. The feedback control law that solves (29) is given by $\widehat{\boldsymbol{u}}_k = -K\boldsymbol{z}_k$ where $K = \left(R_z + B_{\text{lift}}^T P B_{\text{lift}}\right)^{-1} B_{\text{lift}}^T P A_{\text{lift}}$ and P satisfies the discrete-time algebraic Riccati equation $P = A_{\text{lift}}^T P A_{\text{lift}} - A_{\text{lift}}^T P B_{\text{lift}} \left(R_z + B^T P B_{\text{lift}}\right)^{-1} B_{\text{lift}}^T P A_{\text{lift}} + Q_z$. The control input is given by $\boldsymbol{u}_k = M(\widehat{\boldsymbol{u}}_k + \widehat{\omega} \times (M \star ((\dot{\widehat{\omega}})^s)))^s$.

VI. Numerical simulations

Simulation studies have been carried out using MATLAB R2020b on an Intel Core i7 2.2GHz processor. The parameters for the rigid body are the same as in [34]. A rigid body with the moment of inertia $\bar{I}^B = \begin{bmatrix} 1 & 0.1 & 0.15 \\ 0.1 & 0.63 & 0.05 \\ 0.15 & 0.05 & 0.85 \end{bmatrix}$ $\mathrm{Kg} \cdot \mathrm{m}^2$ and mass $m = 1$kg is chosen. The rigid body is positioned at initial position $[x, y, z]^{\mathrm{T}} = [2, 2, 1]^{\mathrm{T}}$m with attitude

LQR cost	Derived observables	Gaussian RBF's
$N=0$	7.9449×10^3	7.9449×10^3
$N=3$	7.5697×10^3	2.1485×10^5
$N=5$	7.0287×10^3	3.2961×10^5

TABLE I: LQR cost versus the number of observables N

$q = [q_1, q_2, q_3, q_4]^{\mathrm{T}} = [0.4618, 0.1917, 0.7999, 0.3320]^{\mathrm{T}}$. The initial linear and angular velocity in the body frame are equal to $\bar{v}^B = [v_x, v_y, v_z]^{\mathrm{T}} = [0.1, -0.2, 0.3]^{\mathrm{T}}\mathrm{m}$ and $\bar{\omega}^B = [p, q, r]^{\mathrm{T}} = [-0.1, 0.2, 0.3]^{\mathrm{T}}$. The task is to steer the rigid body from the given initial state to the origin in the inertial frame. For LQR control design purposes, we take $Q_z = \mathtt{blkdiag}(5\mathbf{I}_{16}, \mathbf{0}_{N-16})$ and $R_z = \mathbf{I}_6$. The values of N_t , N_{total}, and the sampling time T are chosen as $500s$, $6000s = 30s/T$, and $0.05s$ respectively. Consequently, the feedback control inputs $\widehat{\boldsymbol{u}}$ computed by solving (29) are added to the nonlinear system. Fig. 2 shows the evolution of angular and linear velocities with time for $N_1 = 30s$. The lifted state space for the LQR based control design is chosen as $\boldsymbol{z} = [\widehat{q}\ \ \widehat{q\omega}\ \ \widehat{q\omega}^2\ \ \widehat{q\omega}^3\ \ \widehat{q\omega}^4\ \ \widehat{q\omega}^5]^{\mathrm{T}}$. As seen from Table I, the LQR cost decreases as the dimension of the lifted space increases which is in agreement with our analysis. It is worth mentioning that, as seen from Table I using, other popular observables like the Gaussian radial basis functions (RBFs) might not always lead to decrease in the LQR cost as N increases.

VII. CONCLUSIONS

In this paper, we derived a set of Koopman based observables for the rigid body dynamics based on the dual quaternion representation which form a sequence of functions that converges pointwise to the zero function. Subsequently, we utilized the lifted linear model induced by these observables to design an LQR controller which turned out to perform in par with benchmark nonlinear controllers for stabilization of rigid body dynamics. In our future work, we plan to utilize the proposed Koopman operator framework to design more sophisticated controllers (such as covariance steering algorithms) for uncertain rigid body dynamics.

REFERENCES

[1] H.-L. Pham, V. Perdereau, B. V. Adorno, and P. Fraisse, "Position and orientation control of robot manipulators using dual quaternion feedback," in *IEEE International Conference on Intelligent Robots and Systems*, 2010, pp. 658–663.

[2] A. Perez, J. M. McCarthy, and B. Bennett, "Dual quaternion synthesis of constrained robots," in *Advances in Robot Kinematics*. Springer, 2002, pp. 443–452.

[3] A. Perez, J. M. McCarthy, and B. Bennett, "Dual quaternion synthesis of constrained robots," in *Advances in Robot Kinematics*. Springer, 2002, pp. 443–452.

[4] X. Wang and C. Yu, "Feedback linearization regulator with coupled attitude and translation dynamics based on unit dual quaternion," in *IEEE ISIC*, 2010, pp. 2380–2384.

[5] D. Han, Q. Wei, Z. Li, and W. Sun, "Control of oriented mechanical systems: A method based on dual quaternion," *IFAC Proceedings Volumes*, vol. 41, no. 2, pp. 3836–3841, 2008.

[6] R. Schlanbusch, A. Loria, and P. J. Nicklasson, "On the stability and stabilization of quaternion equilibria of rigid bodies," *Automatica*, vol. 48, no. 12, pp. 3135–3141, 2012.

[7] L. F. da Cruz Figueredo, B. V. Adorno, and J. Y. Ishihara, "Robust H_∞ kinematic control of manipulator robots using dual quaternion algebra," *Automatica*, vol. 132, p. 109817, 2021.

[8] J. Wang and Z. Sun, "6-dof robust adaptive terminal sliding mode control for spacecraft formation flying," *Acta Astronautica*, vol. 73, pp. 76–87, 2012.

[9] D. Gan, Q. Liao, S. Wei, J. Dai, and S. Qiao, "Dual quaternion-based inverse kinematics of the general spatial 7r mechanism," *Proceedings of the Institution of Mechanical Engineers, Part C: Journal of Mechanical Engineering Science*, vol. 222, no. 8, pp. 1593–1598, 2008.

[10] Y. Susuki and I. Mezic, "Nonlinear Koopman modes and coherency identification of coupled swing dynamics," *IEEE Transactions on Power Systems*, vol. 26, no. 4, pp. 1894–1904, 2011.

[11] A. Surana, "Koopman operator framework for time series modeling and analysis," *J. Nonlinear Sci.*, pp. 1–34, 2018.

[12] M. Budišić, R. Mohr, and I. Mezić, "Applied Koopmanism," *Chaos*, vol. 22, no. 4, p. 047510, 2012.

[13] B. Lusch, J. N. Kutz, and S. L. Brunton, "Deep learning for universal linear embeddings of nonlinear dynamics," *Nature communications*, vol. 9, no. 1, pp. 1–10, 2018.

[14] S. E. Otto and C. W. Rowley, "Linearly recurrent autoencoder networks for learning dynamics," *SIAM Journal on Applied Dynamical Systems*, vol. 18, no. 1, pp. 558–593, 2019.

[15] E. Yeung, S. Kundu, and N. Hodas, "Learning deep neural network representations for Koopman operators of nonlinear dynamical systems," in *ACC 2019*, 2019, pp. 4832–4839.

[16] M. Haseli and J. Cortés, "Fast identification of Koopman-invariant subspaces: parallel symmetric subspace decomposition," in *2020 American Control Conference (ACC)*, 2020, pp. 4545–4550.

[17] M. Haseli and J. Cortés, "Learning koopman eigenfunctions and invariant subspaces from data: symmetric subspace decomposition," *IEEE Transactions on Automatic Control*, 2021.

[18] M. Haseli and J. Cortés, "Parallel learning of Koopman eigenfunctions and invariant subspaces for accurate long-term prediction," *IEEE Transactions on Control of Network Systems*, 2021.

[19] I. Abraham and T. D. Murphey, "Active learning of dynamics for data-driven control using Koopman operators," *IEEE Transactions on Robotics*, vol. 35, no. 5, pp. 1071–1083, 2019.

[20] D. Bruder, X. Fu, R. B. Gillespie, C. D. Remy, and R. Vasudevan, "Data-driven control of soft robots using Koopman operator theory," *IEEE Transactions on Robotics*, 2020.

[21] G. Mamakoukas, M. L. Castano, X. Tan, and T. D. Murphey, "Derivative-based Koopman operators for real-time control of robotic systems," *IEEE Transactions on Robotics*, 2021.

[22] G. Mamakoukas, M. Castano, X. Tan, and T. Murphey, "Local Koopman operators for data-driven control of robotic systems," in *Robotics: Science and Systems*, 2019.

[23] C. Folkestad, Y. Chen, A. D. Ames, and J. W. Burdick, "Data-driven safety-critical control: Synthesizing control barrier functions with Koopman operators," *IEEE Control Systems Letters*, vol. 5, no. 6, pp. 2012–2017, 2020.

[24] D. Goswami and D. A. Paley, "Bilinearization, reachability, and optimal control of control-affine nonlinear systems: A Koopman spectral approach," *IEEE Transactions on Automatic Control*, 2021.

[25] B. Huang, X. Ma, and U. Vaidya, "Feedback stabilization using Koopman operator," in *2018 IEEE Conference on Decision and Control (CDC)*, 2018, pp. 6434–6439.

[26] T. Chen and J. Shan, "Koopman-operator-based attitude dynamics and control on so (3)," *Journal of Guidance, Control, and Dynamics*, vol. 43, no. 11, pp. 2112–2126, 2020.

[27] V. Zinage and E. Bakolas, "Far-field minimum-fuel spacecraft rendezvous using Koopman operator and l 2/l 1 optimization," in *2021 American Control Conference (ACC)*, 2021, pp. 2992–2997.

[28] Y. Susuki and I. Mezić, "Nonlinear Koopman modes and power system stability assessment without models," *IEEE Transactions on Power Systems*, vol. 29, no. 2, pp. 899–907, 2013.

[29] Y. Susuki and I. Mezic, "Nonlinear Koopman modes and a precursor to power system swing instabilities," *IEEE Transactions on Power Systems*, vol. 27, no. 3, pp. 1182–1191, 2012.

[30] S. Peitz and S. Klus, "Koopman operator-based model reduction for switched-system control of PDEs," *Automatica*, vol. 106, pp. 184–191, 2019.

[31] A. Navarra, J. Tribbia, and S. Klus, "Estimation of Koopman transfer operators for the equatorial pacific sst," *Journal of the Atmospheric Sciences*, vol. 78, no. 4, pp. 1227–1244, 2021.

[32] M. Korda and I. Mezić, "Linear predictors for nonlinear dynamical systems: Koopman operator meets model predictive control," *Automatica*, vol. 93, pp. 149–160, 2018.

[33] N. Filipe and P. Tsiotras, "Simultaneous position and attitude control without linear and angular velocity feedback using dual quaternions," in *American Control Conference*, 2013, pp. 4808–4813.

[34] N. Filipe and P. Tsiotras, "Rigid body motion tracking without linear and angular velocity feedback using dual quaternions," in *2013 European Control Conference (ECC)*, 2013, pp. 329–334.